

The Synthesis and Biological Evaluation of Indolactam Alkaloids

Manuel Mendoza^a

Ryan Eom^b

Celeste Salas^a

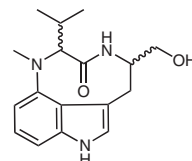
Jeremy Haynes-Smith^c

Kelvin L. Billingsley^{*a} 

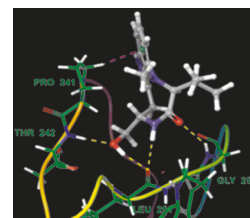
^a Department of Chemistry and Biochemistry, California State University Fullerton, Fullerton, CA 92831, USA
kbillingsley@fullerton.edu

^b Department of Chemistry and Chemical Biology, Cornell University, Ithaca, NY 14853, USA

^c Department of Chemistry and Biochemistry, San Francisco State University, San Francisco, CA 94132, USA



EC₅₀ = 142 nM to >10 μM



Received: 17.07.2019
Accepted after revision: 13.08.2019

Published online: 30.08.2019
DOI: 10.1055/s-0039-1690198; Art ID: ss-2019-m0395-op

Abstract In this work, we execute a general synthetic strategy to access novel indolactam alkaloids, which are agonists of protein kinase C. This protocol allowed for the most efficient reported syntheses of indolactam V (ILV) stereoisomers, while also affording the large-scale production of natural product (-)-ILV. Structure–activity studies were conducted with these compounds to elucidate the elements necessary to promote PKC-mediated cellular response. EC₅₀ measurements in leukemia and lymphoma cell lines, as well as molecular docking analyses with the PKCδ C1B domain, provided the foundation for these studies. A distinct correlation between *in vitro* activity and the conformation of the macrocyclic lactam ring was discovered, which can guide design efforts for therapeutics that target the PKC regulatory domain.

Key words natural products, synthesis, indolactams, amino acids, protein kinase C

Protein kinase C (PKC) is a family of enzymes that participate in an assortment of biochemical networks.¹ Disruption of cell signaling pathways by misregulated PKC activity is associated with numerous pathologies including aggressive tumor promotion in a myriad of cancers.² Over the past decades, the discovery of high-affinity small-molecule PKC binders has furnished scaffolds to fashion molecules for therapeutic intervention. These agonists have also provided powerful tools to interrogate the fundamental biochemical pathways involved in pathogenic PKC function.³

The indolactam alkaloids are a structurally unique family that mimics the behavior of the endogenous PKC activator, diacylglycerol (Figure 1). These natural products have played a critical role in mechanistic investigations of PKC-mediated human disease.⁴ The indolactams are proposed to bind to the PKC regulatory C1 domain through several atoms: the C11 carbonyl, the amide NH, and the C14 primary alcohol.⁵ This pharmacophoric model is further supported

by the fact that (-)-teleocidin B-1 and (-)-indolactam V (**1**), which lacks substitution at C6 and C7, are both potent PKC activators.⁶ Numerous synthetic studies have correspondingly focused on the preparation of **1**,⁷ as this structure possesses the core indolactam motif necessary to promote biological activity.

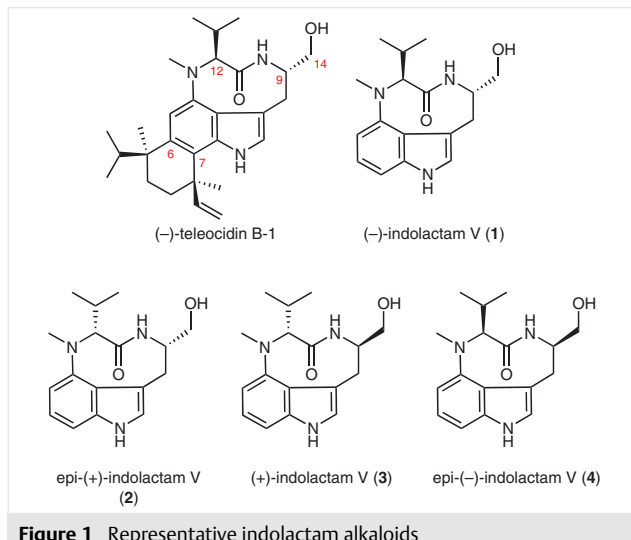


Figure 1 Representative indolactam alkaloids

The stereochemical elements of **1** that are necessary to promote efficient PKC activation have been considered,⁸ and a few reports have detailed methods to access indolactam stereoisomers **2–4**.^{7a,9} Endo and co-workers described an early strategy for the preparation of all four stereoisomers.^{7a,9a} However, several challenges plagued this synthetic route: (1) lengthy synthesis (16 steps) for each stereoisomer, (2) a low-yielding (<20%) nitration for the first step in the sequence, and (3) lack of stereocontrol for establishing the configuration of each stereocenter, leading to multiple

separations of diastereomers. In 2013, a more efficient palladium-catalyzed strategy was employed to prepare **2** and **4** in nine steps, but this route still required three additional transformations (12 total steps) for the preparation of natural product **1**.^{9c} Along with these synthetic achievements, an initial biological study found that although diastereomers of **1** (i.e., **2** and **4**) were inactive in a cell adhesion assay employing the HL-60 leukemia cell line, **3** (enantiomer of **1**) remained active, albeit with a two orders of magnitude reduction in potency.⁸ Interestingly, more recent pre-clinical studies have suggested that **3** possesses enhanced medicinal properties, as it was concluded that **3** possesses increased neuroprotective effects with decreased neurotoxicity relative to natural product **1**.¹⁰

A core long-term objective of our research program is to determine the structural features that govern the biological profile of indolactams in order to increase the therapeutic relevance of this family of PKC activators.

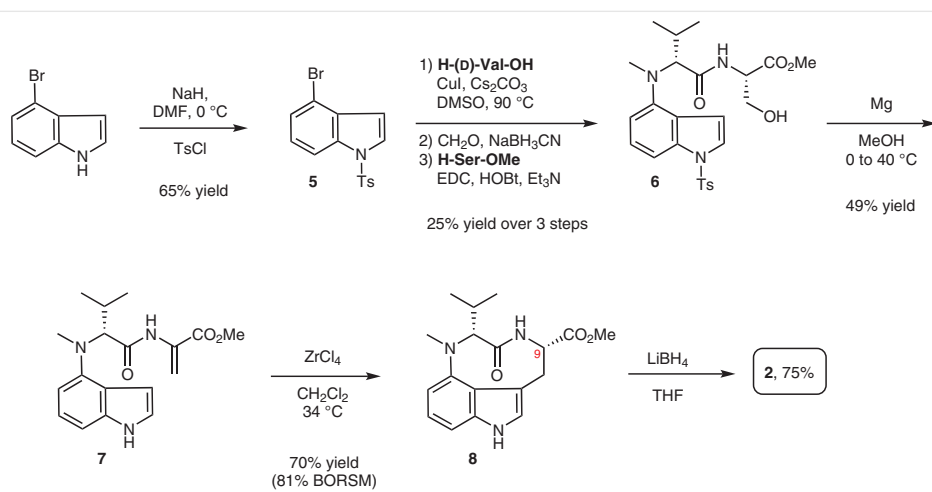
Because the configurations of the C9 and C12 stereocenters in **1** have been proposed to affect the conformation of the nine-membered ring,¹¹ we envisioned that efficient syntheses of indolactam stereoisomers would provide opportunities to fully explore their therapeutic potential and concurrently understand their interactions with the enzymatic target, PKC. To this end, this report describes the implementation of a robust synthetic strategy that selectively affords the analogues **2–4**. Cell-based assays in combination with docking analyses are further employed to elucidate the key elements of indolactam alkaloids that confer PKC-mediated activity.

In an effort to evaluate the biological profile of indolactam stereoisomers, we adapted our synthetic strategy to prepare epi-(+)-indolactam V (**2**).^{7n,12} The synthesis of **2** began with the tosyl protection of 4-bromoindole (Scheme 1). This transformation was performed on a 20 g scale and afforded **5** in a 65% yield upon recrystallization of the crude

material. Dipeptide **6** was then prepared via a three-step sequence (25% yield over three steps) involving the copper-catalyzed arylation of D-valine (H-D-Val-OH) with **5**, reductive amination, and subsequent peptide coupling with L-serine methyl ester (H-Ser-OMe). Because of the instability of the intermediates *en route* to **6**, these reactions were performed in succession without purification after the first and second steps.

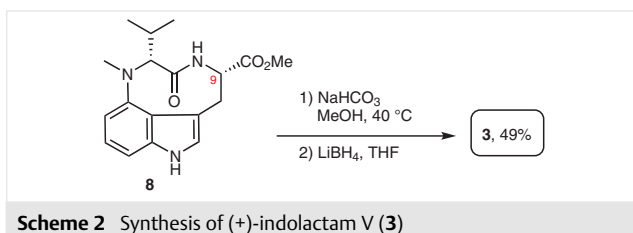
The subsequent transformation was a more problematic magnesium-mediated deprotection–dehydration, which resulted in several byproducts originating from alkene reduction, ester hydrolysis, inefficient deprotection, and decomposition. Increasing magnesium equivalents or concentration had a deleterious effect. Through optimization, we discovered that *N*-tosyl deprotection occurred in near quantitative yield when the reaction was maintained at 0 °C for 4 hours. In the same pot, dehydration could then be accomplished by warming the reaction to 40 °C for 3 hours. This protocol minimized the presence of byproducts and thus provided **7** in a 49% yield. Lewis acid catalyzed cyclization¹³ of **7** afforded **8** in a 70% yield (81% yield based on recovered starting material) with no other stereoisomers observed.^{7j,n} The high level of selectivity in this transformation suggests a conformational preference induced by the C12 stereocenter, and we are currently undertaking investigations to elucidate the origins of this stereoselectivity. Epi-(+)-indolactam V (**2**) was finally prepared through the direct reduction of intermediate **8** (Scheme 1). Importantly, this seven-step route is the shortest reported process for obtaining an epimer of natural product **1**. In addition, our sequence does not require time-consuming and difficult separations of diastereomeric mixtures, which plagues previous works.

(+)-Indolactam V (**3**) differs from **2** in the configuration at the C9 stereocenter; therefore, tricycle **8** could be converted into **3** by a protocol of C9 epimerization with weak



Scheme 1 Synthesis of epi-(+)-indolactam V (**2**)

base followed by ester reduction (Scheme 2). Although the epimerization resulted in a ~1:1 ratio of diastereomers (desired product vs starting material), our synthesis of **3** represents the most efficient protocol for the preparation of this potential therapeutically relevant molecule.

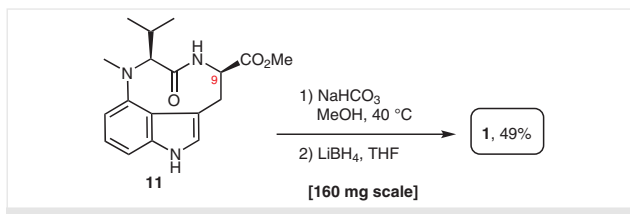


Scheme 2 Synthesis of (+)-indolactam V (3)

Epi-(–)-indolactam V (**4**) was prepared through application of our general strategy to access these alkaloids (Scheme 3). To establish the C12 configuration, L-valine (H-Val-OH) was subjected to the copper-catalyzed aminoarylation with starting material **5** and, similarly, reductive amination followed by peptide coupling with H-Ser-OMe afforded dipeptide **9**. This intermediate smoothly underwent magnesium-promoted deprotection–dehydration to yield **10** and then cyclization to afford **11**. Direct reduction of **11** (70% yield) completed the synthesis of stereoisomer **4** in seven total transformations.

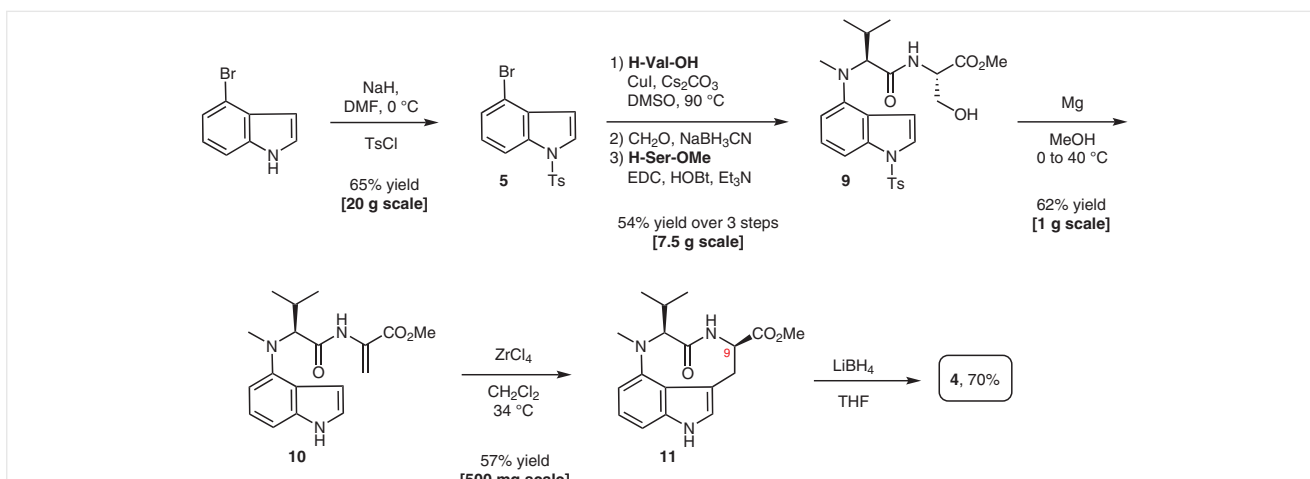
In addition to these studies on the indolactam stereoisomers, our continuing synthetic goal is to establish a modular process for preparing teleocidin-inspired bioactive agents, which have substitution at the C6 and/or C7 position of the scaffold. This objective further necessitates a scalable synthesis of **1**. Because the intermediates *en route* to **4** are consistent with the synthesis of **1**, we demonstrated each of these transformations to prepare tricycle **11** on larger scales (Scheme 3) using our optimized protocols. Similar to its enantiomer, **11** successfully underwent base-

induced epimerization at C9 to yield the corresponding diastereomer. Because a difficult column chromatographic separation must be conducted to isolate the material, the epimerization process is typically performed on ≤200 mg scale batches. Overall, **1** was prepared in a 49% yield from **11** by the C9 epimerization–reduction sequence (Scheme 4). Our optimized route has yielded >500 mg of **1** for further synthetic studies. Overall, our synthetic strategy offered practical and selective syntheses of all indolactam V stereoisomers, which could then be transitioned to biological studies.



Scheme 4 Scale-up of (–)-indolactam V (1)

PKC regulatory domain activators have been examined as potential cancer therapeutics in numerous clinical trials.¹⁴ The majority of these studies rely upon the natural product bryostatin 1, and leukemia and lymphoma have historically been the primary cancers targeted. To determine the activity of the indolactam natural product and analogues, cell growth inhibition assays were conducted with two human cancer cell lines: K562 (chronic myelogenous leukemia) and U937 (histiocytic lymphoma). Bryostatin 1 was also examined simultaneously as a comparison. In the K562 cell line, (–)-indolactam V (**1**) had an EC₅₀ value of 143 ± 75 nM (Figure 2).¹² Interestingly, **1** displayed a significant increase ($p = 0.0064$, *t* test) in activity relative to bryostatin 1 (640 ± 76 nM). Indolactam V stereoisomers **2**–**4** did not produce growth inhibitory effects in the concentration



Scheme 3 Synthesis of epi-(–)-indolactam V (4)

range evaluated. Similar trends were detected in the U937 lymphoma cell line. Bryostatin 1 yielded an $EC_{50} = 111 \pm 39$ nM, which was statistically similar to measurements obtained for **1** (142 ± 36 nM). Indolactam V stereoisomers **2–4** again showed diminished activity relative to **1**, and $>10 \mu\text{M}$ EC_{50} values were obtained with these analogues in both cancer cell lines. Overall, these assays provided several key insights and verifications: (1) **1** can display *in vitro* activity measurements comparable to bryostatin 1, (2) enantiomer **3**, unlike previous reports, is inactive in several key cancer cell lines at micromolar concentrations, and (3) alterations of the natural configurations at the C9 or C12 stereocenters renders the compound unable to promote a PKC-mediated biological response.

Compound	Cancer cell lines EC_{50} (nM) ^a	
	K562 ^b	U937 ^c
bryostatin 1	640 \pm 76	111 \pm 39
1	143 \pm 75	142 \pm 36
2	$>10,000$	$>10,000$
3	$>10,000$	$>10,000$
4	$>10,000$	$>10,000$

Figure 2 Cell growth inhibition data for assays of synthesized and standard compounds with cancer cell lines K562 and U937. ^a EC_{50} values are the average of at least three experiments; experimental error indicates standard error of the mean. ^b Human chronic myelogenous leukemia cell line. ^c Human histiocytic lymphoma cell line.

Molecular docking analyses were performed with **1–4** and the PKC δ C1B domain to further elucidate the observed differences in activity. Natural product **1** exists as a mixture of two conformers (twist vs sofa) at room temperature.^{7b} The twist conformation possesses a *cis*-amide in the nine-membered ring, whereas the sofa conformation establishes a *trans*-amide geometry. A *cis*-amide has been proposed to be a necessary component for efficient binding to the C1 regulatory domain.¹⁵

Docking simulation of **1** with the twist conformation and the PKC δ C1B domain was conducted using the program Schrödinger Maestro (Figure 3). Traditional hydrogen-bonding contacts were observed between the indolactam

pharmacophore and key amino acids (Thr-242, Leu-251, Gly-253).¹⁶ In addition, the indole ring of **1** was in proximity to the hydrogen atom of Pro-241 (2.64 Å), allowing for a potential stabilizing CH/ π interaction.¹⁶

Early reports speculated that epimers of **1** might adopt a different geometry for the nine-membered macrocycle.^{7b} It is now believed **2** and **4** exist in a single conformation at room temperature, and this conformer also possesses a *cis*-amide configuration.¹⁷ This geometry promotes a distortion of the nine-membered lactam ring, where distances between the hydrogens at C9 and C12 are 2.1 Å versus a distance of 4.0 Å in the standard twist conformation. To clarify whether these geometric constraints affect the binding to the receptors, simulations were also performed with **2** and **4** (Figure 3). Docking of these indolactam V stereoisomers resulted in a reduced number of interactions with the C1B domain. For example, **2** did not maintain the Pro-241 CH/ π interaction found in natural product **1**. No binding modes for **4** allowed for either the CH/ π interaction or the maximum amount of hydrogen-bonding contacts. This decrease in efficiency of docking to the PKC regulatory domain is in agreement with the reduced activity observed in the cell growth inhibition assays. In addition, although the enantiomer of **1** (i.e., **3**) adopts a twist geometry, no successfully docked structures were found and correspondingly low activity values were detected in the biological analyses. The lack of an efficient binding mode for **3** provides a preliminary indication that neuroprotective effects detected with the compound in previous reports¹⁰ may not be directly PKC-mediated.

In summary, we have developed a concise synthetic route to access indolactams. This work represents the most efficient sequence, to date, to prepare all indolactam V stereoisomers. These advancements provided the opportunity for examination of the stereochemical elements of the indolactam core that dictate PKC-mediated activity. The naturally occurring indolactam maintained a higher level of potency in two cancer cell lines, and subsequent docking studies suggested that stereoisomers of **1** exist in conformations that limit their potential for efficient binding to the PKC C1 regulatory domain.

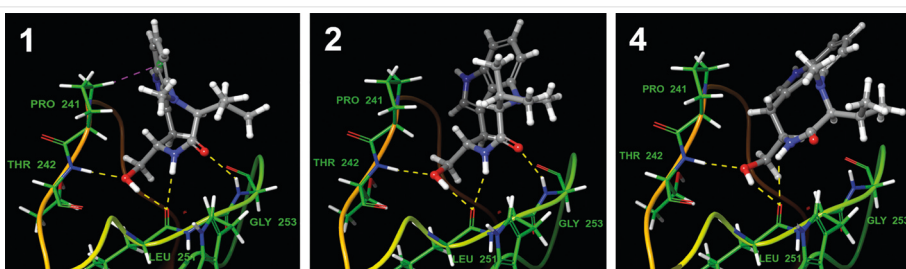


Figure 3 Docking simulation for indolactams **1**, **2** and **4** with the PKC δ C1B domain. No energetically favorable conformations were found for (+)-indolactam V (**3**).

Unless otherwise noted, all reactions were performed under an air atmosphere in oven-dried glassware. Commercially available reagents were purchased from Sigma-Aldrich and used without further purification. Reactions were stirred using Teflon-coated magnetic stirrer bars. Reactions were monitored via TLC using 0.25 mm silica gel 60F plates with fluorescent indicator. Plates were visualized under UV light without further staining. Products were purified via column chromatography using silica gel 60, 230–400 mesh and the solvent system(s) indicated. Known compounds were characterized by ¹H NMR spectroscopy and compared to the literature. All new compounds were characterized by ¹H and ¹³C NMR spectroscopy and high-resolution mass spectrometry. NMR spectra were measured on a Bruker 400 (¹H at 400 MHz, ¹³C at 100 MHz) magnetic resonance spectrometer. ¹H chemical shifts are reported relative to the residual solvent peak (chloroform = 7.26 ppm) or TMS (0.0 ppm) as follows: chemical shift (δ), (multiplicity (s = singlet, bs = broad singlet, d = doublet, dd = doublet of doublets, t = triplet, q = quartet), coupling constant(s) in Hz, integration). ¹³C chemical shifts are reported relative to the deuterated solvent ¹³C signals (chloroform = 77 ppm) or TMS (0.0 ppm). High-resolution mass spectra were obtained using ultra performance liquid chromatography–mass spectrometry (UPLC-MS). Melting points were obtained on a Mel-Temp capillary melting point apparatus.

4-Bromo-1-tosyl-1H-indole (5)

An oven-dried round-bottom flask equipped with a magnetic stir bar was charged with 4-bromoindole (20 g, 102 mmol). The flask was sealed with a septum, and a balloon with needle was inserted through the septum. DMF (200 mL) was added via syringe through the septum and the reaction was cooled to 0 °C with an ice bath. NaH (60%) (4.88 g, 122 mmol) was added directly to the flask in one portion. NOTE: necessary safety precautions should be taken when employing NaH with DMF on larger scales.¹⁸ The reaction was allowed to warm to rt over 45 min followed by re-cooling to 0 °C. Tosyl chloride (28.8 g, 153 mmol) in DMF (120 mL) was added via syringe over 2 min. The reaction was allowed to warm to rt overnight (15 h). The crude reaction mixture was diluted with H₂O (400 mL). The resulting solution was extracted with EtOAc (1 L). The organic layer was separated. The aqueous layer was extracted with EtOAc (2 × 500 mL). The combined organic layers were dried with MgSO₄, filtered and concentrated to yield a brown oil. Recrystallization (EtOAc/hexanes) provided **5** as a light brown solid; yield: 23.2 g (65%). Characterization data matched previously reported information.⁷ⁿ

¹H NMR (400 MHz, CDCl₃): δ = 7.96 (d, J = 8 Hz, 1 H), 7.76 (d, J = 8 Hz, 2 H), 7.63 (d, J = 2 Hz, 1 H), 7.38 (d, J = 8 Hz, 1 H), 7.19–7.23 (m, 2 H), 7.17 (t, J = 8 Hz, 1 H), 6.72 (d, J = 3 Hz, 1 H), 2.32 (s, 3 H).

Methyl N-Methyl-N-(1-tosyl-1H-indol-4-yl)-D-valyl-L-serinate (6)

An oven-dried Schlenk flask equipped with a magnetic stir bar was charged with Cul (108 mg, 0.57 mmol), D-valine (800 mg, 6.8 mmol), **5** (2.00 g, 5.7 mmol) and Cs₂CO₃ (2.78 g, 8.5 mmol). The flask was capped with a septum and then evacuated and backfilled with argon (this sequence was carried out three times). DMSO (11.4 mL) was added via syringe through the septum. Under an argon atmosphere, the septum was replaced and sealed with a Teflon screwcap. The reaction was heated to 90 °C for 20 h, then cooled to rt and filtered through a pad of silica gel eluting with MeOH. The solution was concentrated under reduced pressure to mostly remove residual DMSO and yield a brown oil that was used directly in the subsequent transformation.

The oil was transferred to a round-bottom flask equipped with a magnetic stir bar and dissolved in CH₃CN (55 mL). Formaldehyde (6.9 mL; 38% solution) was added to the stirring solution via syringe. After 5 min, NaBH₃CN (1.64 g, 26.1 mmol) was added directly to the flask followed by the dropwise addition of AcOH (1.75 mL) over 1 min. The reaction was allowed to stir for 1 h at rt. The crude reaction mixture was diluted with H₂O (30 mL). The resulting solution was extracted with EtOAc (50 mL). The organic layer was separated. The aqueous layer was extracted with EtOAc (2 × 50 mL). The combined organic layers were concentrated to yield a light brown oil that was used directly in the subsequent transformation.

L-Serine methyl ester hydrochloride (1.33 g, 8.5 mmol) was charged into an oven-dried round-bottom flask equipped with a magnetic stir bar, and dissolved in CH₂Cl₂ (45 mL). Et₃N (3.13 mL, 2.27 g, 22.4 mmol) was added via syringe. The reaction was allowed to stir at rt for 30 min and then cooled to 0 °C with an ice bath. Hydroxybenzotriazole hydrate (1.04 g, 7.7 mmol) was added directly to the flask followed by the addition of the starting material dissolved in CH₂Cl₂ (12.5 mL) (an additional 0.50 mL used to ensure all material was transferred to the reaction flask). 1-Ethyl-3-(3-dimethylaminopropyl)carbodiimide hydrochloride (EDC; 1.30 g, 8.4 mmol) was then added directly to the flask. The reaction was allowed to stir at rt overnight (15 h). The crude reaction mixture was diluted with H₂O (30 mL). The resulting solution was extracted with CH₂Cl₂ (30 mL). The organic layer was separated. The aqueous layer was extracted with CH₂Cl₂ (2 × 30 mL). The combined organic layers were dried with MgSO₄, filtered and concentrated. Purification by flash column chromatography (55% EtOAc/hexanes) afforded **6** as a colorless solid; yield: 700 mg (25%); mp 34–36 °C.

¹H NMR (400 MHz, CDCl₃): δ = 7.76 (d, J = 8 Hz, 2 H), 7.64 (d, J = 8 Hz, 1 H), 7.54 (d, J = 4 Hz, 1 H), 7.18–7.25 (m, 3 H), 6.83 (d, J = 8 Hz, 1 H), 6.77 (d, J = 4 Hz, 1 H), 6.44 (d, J = 8 Hz, 1 H), 4.50 (m, 1 H), 3.79 (d, J = 8 Hz, 1 H), 3.72 (dd, J = 4, 12 Hz, 1 H), 3.67 (s, 3 H), 3.58 (dd, J = 4, 12 Hz, 1 H), 2.87 (s, 3 H), 2.42 (m, 1 H), 2.35 (s, 3 H), 2.09 (bs, 1 H), 1.10 (d, J = 8 Hz, 3 H), 1.01 (d, J = 8 Hz, 3 H).

¹³C NMR (100 MHz, CDCl₃): δ = 170.8, 170.4, 145.7, 145.0, 136.2, 135.2, 129.9, 126.9, 125.3, 125.0, 123.7, 113.0, 107.8, 107.0, 71.9, 63.1, 54.2, 52.5, 36.0, 27.7, 21.5, 19.8, 19.4.

HRMS-ESI+: *m/z* calcd for C₂₅H₃₁N₃O₆S + H: 502.2012; found: 502.2008.

Methyl (R)-2-(2-((1H-Indol-4-yl)(methyl)amino)-3-methylbutan-amido)acrylate (7)

An oven-dried reaction tube equipped with a magnetic stir bar was charged with **6** (47 mg, 0.094 mmol). MeOH (2.4 mL) was added directly to the tube followed by the addition of magnesium turnings (24 mg, 0.97 mmol). The tube was cooled to 0 °C with an ice bath and the mixture allowed to stir for 4 h. After this time, the reaction mixture was heated to 40 °C and stirred for an additional 3 h. The crude reaction mixture was diluted with aq NH₄Cl (10 mL). The resulting solution was extracted with EtOAc (12 mL). The organic layer was separated. The aqueous layer was extracted with EtOAc (2 × 12 mL). The combined organic layers were dried with MgSO₄, filtered and concentrated. The crude product was further purified by flash column chromatography (25% EtOAc/hexanes) to afford **7** as a colorless oil; yield: 15.3 mg (49%).

¹H NMR (400 MHz, CDCl₃): δ = 8.30 (bs, 1 H), 8.11 (bs, 1 H), 7.16 (t, J = 3 Hz, 1 H), 7.06–7.13 (m, 2 H), 6.67 (d, J = 7 Hz, 1 H), 6.63 (m, 1 H), 6.58 (s, 1 H), 5.83 (s, 1 H), 4.13 (t, J = 8 Hz, 1 H), 3.69 (s, 3 H), 2.90 (s, 3 H), 2.45 (m, 1 H), 1.15 (d, J = 8 Hz, 3 H), 1.03 (d, J = 8 Hz, 3 H).

¹³C NMR (100 MHz, CDCl₃): δ = 170.2, 164.0, 144.5, 137.4, 130.7, 122.9, 122.7, 120.6, 109.3, 108.6, 105.9, 101.1, 72.3, 52.7, 36.0, 27.6, 19.9, 19.8.

HRMS-ESI+: *m/z* calcd for C₁₈H₂₃N₃O₃ + H: 330.1818; found: 330.1806.

Methyl (2*R*,5*S*)-2-Isopropyl-1-methyl-3-oxo-2,3,4,5,6,8-hexahydro-1*H*-[1,4]diazonino[7,6,5-*cd*]indole-5-carboxylate (8)

An oven-dried reaction tube equipped with a magnetic stir bar was charged with **7** (60 mg, 0.18 mmol). The reaction tube was transferred into a glovebox. ZrCl₄ (634 mg, 2.7 mmol) and then CH₂Cl₂ (1.85 mL) were added. The reaction tube was sealed, transferred out of the glovebox and then heated to 34 °C. After 24 h, the reaction mixture was cooled to rt and then added dropwise to saturated aq NaHCO₃ (3 mL) at 0 °C. The resulting solids were removed by filtration over Celite (EtOAc eluent). The layers were separated and the aqueous layer was extracted with EtOAc. The combined organic layers were dried over MgSO₄. Concentration under reduced pressure afforded the crude product, which was purified by flash chromatography (40% EtOAc/hexanes) to afford recovered starting material **7** (10 mg, 16% recovered) and **8** as a colorless solid; yield: 42 mg (70%); mp 136–138 °C.

¹H NMR (400 MHz, CDCl₃): δ = 8.03 (bs, 1 H), 7.05 (t, *J* = 8 Hz, 1 H), 7.00 (d, *J* = 2 Hz, 1 H), 6.96 (d, *J* = 8 Hz, 1 H), 6.78 (d, *J* = 8 Hz, 1 H), 6.66 (d, *J* = 8 Hz, 1 H), 4.49 (m, 1 H), 3.92 (s, 3 H), 3.80 (d, *J* = 11 Hz, 1 H), 3.46 (dd, *J* = 4, 8 Hz, 1 H), 3.31 (d, *J* = 4 Hz, 1 H), 3.12 (s, 3 H), 2.66 (m, 1 H), 0.75 (d, *J* = 8 Hz, 3 H), 0.70 (d, *J* = 8 Hz, 3 H).

¹³C NMR (100 MHz, CDCl₃): δ = 172.5, 172.4, 148.0, 138.4, 122.7, 122.6, 120.4, 113.3, 109.7, 105.4, 69.8, 57.3, 53.1, 35.1, 32.4, 28.5, 20.5, 20.0.

HRMS-ESI+: *m/z* calcd for C₁₈H₂₃N₃O₃ + H: 330.1818; found: 330.1814.

Epi-(+)-indolactam V (2)

8 (8.5 mg, 0.027 mmol) was charged into an oven-dried reaction tube equipped with a magnetic stir bar. The reaction tube was transferred into a glovebox. LiBH₄ (5.8 mg, 0.27 mmol) and then THF (150 μ L) were added. The reaction tube was sealed, transferred out of the glovebox and then allowed to stir at rt. After 5 h, the reaction mixture was added to H₂O (0.50 mL) at 0 °C. The resulting solution was extracted with CH₂Cl₂ (1 mL). The organic layer was separated. The aqueous layer was extracted with CH₂Cl₂ (2 \times 1 mL). The combined organic layers were dried with MgSO₄, filtered and concentrated under reduced pressure. The crude product was further purified by flash chromatography (70% EtOAc/hexanes) to afford **2** as a colorless solid; yield: 6.0 mg (75%); mp 105–107 °C. Characterization data matched previously reported information.^{9c}

¹H NMR (400 MHz, CDCl₃): δ = 8.00 (bs, 1 H), 7.54 (bs, 1 H), 7.06 (d, *J* = 7 Hz, 1 H), 6.97 (d, *J* = 7 Hz, 1 H), 6.89 (d, *J* = 2 Hz, 1 H), 6.77 (d, *J* = 7 Hz, 1 H), 3.98 (d, *J* = 10 Hz, 1 H), 3.79–3.95 (m, 3 H), 3.27 (d, *J* = 16 Hz, 1 H), 3.13 (s, 3 H), 2.95 (d, *J* = 16 Hz, 1 H), 2.64 (m, 1 H), 0.76 (d, *J* = 7 Hz, 3 H), 0.71 (d, *J* = 7 Hz, 3 H).

¹³C NMR (100 MHz, CDCl₃): δ = 175.2, 148.0, 138.5, 122.4, 122.1, 120.5, 114.1, 109.4, 105.3, 68.9, 65.4, 57.6, 32.5, 29.7, 28.3, 20.3, 20.0.

HRMS-ESI+: *m/z* calcd for C₁₇H₂₃N₃O₂ + H: 302.1869; found: 302.1864.

(+)-Indolactam V (3)

An oven-dried reaction tube equipped with a magnetic stir bar was charged with **8** (19.0 mg, 0.058 mmol). MeOH (3.9 mL) was added followed by NaHCO₃ (134 mg, 1.60 mmol). The reaction tube was sealed and heated to 40 °C. After 72 h, the reaction mixture was cooled to rt, concentrated and partitioned between EtOAc (10 mL) and H₂O (10 mL). The organic layer was removed and the aqueous layer was extracted with EtOAc (3 \times 10 mL). The combined organic layers were dried with MgSO₄, filtered and concentrated. The crude product was purified by flash column chromatography (10% CH₃CN/benzene) to afford the epimer product (9.5 mg, 50% yield) as a colorless solid and recovered starting material **8** (8.6 mg, 45% recovered).

The epimer (6.1 mg, 0.019 mmol) was charged into an oven-dried reaction tube equipped with a magnetic stir bar. The reaction tube was transferred into a glovebox. LiBH₄ (4.0 mg, 0.19 mmol) and then THF (150 μ L) were added. The reaction tube was sealed, transferred out of the glovebox and then allowed to stir at rt. After 5 h, the reaction mixture was added to H₂O (0.50 mL) at 0 °C. The resulting solution was extracted with CH₂Cl₂ (1 mL). The organic layer was separated. The aqueous layer was extracted with CH₂Cl₂ (2 \times 1 mL). The combined organic layers were dried with MgSO₄, filtered and concentrated under reduced pressure. The crude product was further purified by flash chromatography (70% EtOAc/hexanes) to afford **3** as a colorless solid; yield: 5.5 mg (99%). Characterization data matched previously reported information.^{7b}

¹H NMR (400 MHz, CDCl₃) showed the presence of two rotamers: δ (major rotamer) = 8.03 (bs, 1 H), 7.32 (bs, 1 H), 7.06 (d, *J* = 8 Hz, 1 H), 6.90 (d, *J* = 8 Hz, 1 H), 6.50 (d, *J* = 8 Hz, 1 H), 4.39 (d, *J* = 10 Hz, 1 H), 4.31 (m, 1 H), 3.75 (d, *J* = 8 Hz, 1 H), 3.57 (m, 1 H), 3.18 (d, *J* = 15 Hz, 1 H), 3.03 (d, *J* = 15 Hz, 1 H), 2.92 (s, 3 H), 2.56–2.65 (m, 1 H), 0.93 (d, *J* = 7 Hz, 3 H), 0.63 (d, *J* = 7 Hz, 3 H).

¹³C NMR (100 MHz, CDCl₃): δ = 174.2, 147.8, 139.4, 122.9, 121.3, 117.9, 114.6, 106.4, 103.9, 71.1, 65.1, 55.8, 34.0, 33.0, 28.5, 21.6, 19.5.

HRMS-ESI+: *m/z* calcd for C₁₇H₂₃N₃O₂ + H: 302.1869; found: 302.1862.

Methyl N-Methyl-N-(1-tosyl-1*H*-indol-4-yl)-L-valyl-L-serinate (9)

An oven-dried Schlenk flask equipped with a magnetic stir bar was charged with CuI (407 mg, 2.14 mmol), valine (6.00 g, 51.2 mmol), **5** (7.50 g, 21.5 mmol) and Cs₂CO₃ (10.4 g, 32.0 mmol). The flask was capped with a septum and then evacuated and backfilled with argon (this sequence was carried out three times). DMSO (42 mL) was added via syringe through the septum. Under an argon atmosphere, the septum was replaced and sealed with a Teflon screwcap. The reaction was heated to 90 °C for 20 h, then cooled to rt and filtered through a pad of silica gel eluting with MeOH. The solution was concentrated under reduced pressure to mostly remove residual DMSO and yield a brown oil that was used directly in the subsequent transformation.

The oil was transferred to a round-bottom flask equipped with a magnetic stir bar, and dissolved in CH₃CN (205 mL). Formaldehyde (25.8 mL; 38% solution) was added to the stirring solution via syringe. The reaction was cooled to 0 °C. After 5 min, NaBH₃CN (6.15 g, 97.9 mmol) and activated 4 Å molecular sieves (25 g) were added directly to the flask followed by the dropwise addition of AcOH (6.56 mL) over 5 min. The reaction was allowed to stir for an additional 5 min at rt. The crude reaction mixture was immediately filtered and diluted with H₂O (120 mL). The resulting solution was extracted with EtOAc (180 mL). The organic layer was separated. The aqueous layer was extracted with EtOAc (2 \times 180 mL). The combined organic layers were dried with MgSO₄, filtered and concentrated to yield a light brown oil that was used directly in the subsequent transformation.

L-Serine methyl ester hydrochloride (14.9 g, 96 mmol) was charged into an oven-dried round-bottom flask equipped with a magnetic stir bar. The flask was sealed with a septum, and a balloon with needle was inserted through the septum. CH_2Cl_2 (164 mL) followed by Et_3N (35.2 mL, 248 mmol) were added consecutively to the stirring solution via syringe. The reaction was allowed to stir at rt for 30 min and then cooled to 0 °C with an ice bath. Hydroxybenzotriazole hydrate (7.78 g, 51 mmol) and activated 4 Å molecular sieves (12 g) were added directly to the flask followed by the addition of the starting material dissolved in CH_2Cl_2 (45 mL) (an additional 6 mL used to ensure all material was transferred to the reaction flask). EDC (9.78 g, 51 mmol) was then added directly to the flask. The reaction was allowed to stir at rt. After 1 h, a second portion of hydroxybenzotriazole hydrate (7.78 g, 51 mmol) and EDC (9.78 g, 51 mmol) was added directly to the flask. The reaction was allowed to stir at rt overnight (15 h). The crude reaction mixture was filtered and then diluted with H_2O (120 mL). The resulting solution was extracted with CH_2Cl_2 (120 mL). The organic layer was separated. The aqueous layer was extracted with CH_2Cl_2 (2 × 120 mL). The combined organic layers were dried with MgSO_4 , filtered and concentrated. Purification by flash column chromatography (55% EtOAc/hexanes) afforded **9** as a colorless solid; yield: 5.79 g (54%). Characterization data matched previously reported information.⁷ⁿ

¹H NMR (400 MHz, CDCl_3): δ = 7.75 (d, J = 8 Hz, 2 H), 7.65 (d, J = 8 Hz, 1 H), 7.56 (d, J = 4 Hz, 1 H), 7.19–7.23 (m, 3 H), 6.79 (d, J = 8 Hz, 1 H), 6.76 (d, J = 4 Hz, 1 H), 5.93 (d, J = 8 Hz, 1 H), 4.53 (m, 1 H), 3.66 (s, 3 H), 3.64–3.74 (m, 2 H), 3.55 (dd, J = 4, 8 Hz, 1 H), 2.84 (s, 3 H), 2.40 (m, 1 H), 2.34 (s, 3 H), 1.67 (bs, 1 H), 1.18 (d, J = 8 Hz, 3 H), 0.96 (d, J = 8 Hz, 3 H).

Methyl (S)-2-(2-((1*H*-Indol-4-yl)(methyl)amino)-3-methylbutan-amido)acrylate (**10**)

An oven-dried reaction tube equipped with a magnetic stir bar was charged with **9** (1.42 g, 2.83 mmol). MeOH (71 mL) was added directly to the tube followed by the addition of magnesium turnings (702 mg, 28.9 mmol). The tube was cooled to 0 °C with an ice bath and the mixture allowed to stir for 4 h. After this time, the reaction mixture was heated to 40 °C and stirred for an additional 3 h. The crude reaction mixture was diluted with aq NH_4Cl (35 mL). The resulting solution was extracted with EtOAc (40 mL). The organic layer was separated. The aqueous layer was extracted with EtOAc (2 × 40 mL). The combined organic layers were dried with MgSO_4 , filtered and concentrated. The crude product was further purified by flash column chromatography (25% EtOAc/hexanes) to afford **10** as a colorless oil; yield: 586 mg (62%). Characterization data matched previously reported information.⁷ⁿ

¹H NMR (400 MHz, CDCl_3): δ = 8.30 (bs, 1 H), 8.11 (bs, 1 H), 7.16 (t, J = 3 Hz, 1 H), 7.06–7.10 (m, 2 H), 6.62–6.67 (m, 2 H), 6.58 (s, 1 H), 5.83 (s, 1 H), 4.13 (t, J = 8 Hz, 1 H), 3.69 (s, 3 H), 2.90 (s, 3 H), 2.45 (m, 1 H), 1.15 (d, J = 8 Hz, 3 H), 1.03 (d, J = 8 Hz, 3 H).

Methyl (2*S*,5*R*)-2-Isopropyl-1-methyl-3-oxo-2,3,4,5,6,8-hexahydro-1*H*-[1,4]diazonino[7,6,5-cd]indole-5-carboxylate (**11**)

An oven-dried Schlenk flask equipped with a magnetic stir bar was charged with **10** (533 mg, 1.62 mmol). The flask was transferred into a glovebox. ZrCl_4 (5.41 g, 23.2 mmol) and then CH_2Cl_2 (15.5 mL) were added. The reaction tube was sealed, transferred out of the glovebox and then heated to 34 °C. After 24 h, the reaction mixture was cooled to rt and then added dropwise to saturated aq NaHCO_3 (225 mL) at 0 °C. The resulting solids were removed by filtration over Celite

(EtOAc eluent). The layers were separated and the aqueous layer was extracted with EtOAc (3 × 225 mL). The combined organic layers were dried over MgSO_4 . Concentration under reduced pressure afforded the crude product, which was further purified by flash chromatography (40% EtOAc/hexanes) to afford **11** as a colorless solid; yield: 303 mg (57%). Characterization data matched previously reported information.⁷ⁿ

¹H NMR (400 MHz, CDCl_3): δ = 8.03 (bs, 1 H), 7.05 (t, J = 8 Hz, 1 H), 7.00 (d, J = 2 Hz, 1 H), 6.96 (d, J = 8 Hz, 1 H), 6.78 (d, J = 8 Hz, 1 H), 6.66 (d, J = 8 Hz, 1 H), 4.49 (t, J = 3 Hz, 1 H), 3.92 (s, 3 H), 3.80 (d, J = 11 Hz, 1 H), 3.46 (dd, J = 3, 3 Hz, 1 H), 3.31 (dd, J = 4, 4 Hz, 1 H), 3.12 (s, 3 H), 2.62–2.69 (m, 1 H), 0.75 (d, J = 7 Hz, 3 H), 0.70 (d, J = 7 Hz, 3 H).

Epi-(–)-indolactam **V** (**4**)

11 (13.9 mg, 0.042 mmol) was charged into an oven-dried reaction tube equipped with a magnetic stir bar. The reaction tube was transferred into a glovebox. LiBH_4 (9.2 mg, 0.42 mmol) and then THF (150 μ L) were added. The reaction tube was sealed, transferred out of the glovebox and then allowed to stir at rt. After 5 h, the reaction mixture was added to H_2O (0.75 mL) at 0 °C. The resulting solution was extracted with CH_2Cl_2 (1.5 mL). The organic layer was separated. The aqueous layer was extracted with CH_2Cl_2 (2 × 1.5 mL). The combined organic layers were dried with MgSO_4 , filtered and concentrated under reduced pressure. The crude product was further purified by flash chromatography (70% EtOAc/hexanes) to afford **4** as a colorless solid; yield: 8.9 mg (70%); mp 108–110 °C. Characterization data matched previously reported information.^{9c}

¹H NMR (400 MHz, CDCl_3): δ = 8.03 (bs, 1 H), 7.75 (bs, 1 H), 7.05 (t, J = 7 Hz, 1 H), 6.97 (d, J = 7 Hz, 1 H), 6.89 (d, J = 2 Hz, 1 H), 6.77 (d, J = 7 Hz, 1 H), 3.98 (d, J = 10 Hz, 1 H), 3.84–3.91 (m, 3 H), 3.26 (d, J = 16 Hz, 1 H), 3.12 (s, 3 H), 2.95 (d, J = 16 Hz, 1 H), 2.63 (m, 1 H), 0.76 (d, J = 7 Hz, 3 H), 0.71 (d, J = 7 Hz, 3 H).

¹³C NMR (100 MHz, CDCl_3): δ = 175.3, 148.0, 138.5, 122.4, 122.2,

120.5, 114.1, 109.4, 105.3, 68.9, 65.4, 57.7, 32.5, 29.7, 28.3, 20.3, 19.9.

HRMS-ESI+: *m/z* calcd for $\text{C}_{17}\text{H}_{23}\text{N}_3\text{O}_2 + \text{H}$: 302.1869; found: 302.1865.

(–)-Indolactam **V** (**1**)

An oven-dried reaction tube equipped with a magnetic stir bar was charged with **11** (160 mg, 0.49 mmol). MeOH (33 mL) was added followed by NaHCO_3 (1.13 g, 13.5 mmol). The reaction tube was sealed and heated to 40 °C. After 72 h, the reaction mixture was cooled to rt, concentrated and partitioned between EtOAc (80 mL) and H_2O (80 mL). The organic layer was removed and the aqueous layer was extracted with EtOAc (3 × 80 mL). The combined organic layers were dried with MgSO_4 , filtered and concentrated. The crude product was purified by flash column chromatography (10% CH_3CN /benzene) to afford the epimer product (80 mg, 50% yield) as a colorless solid and recovered starting material **11** (71 mg, 44% recovered).

The epimer (80 mg, 0.24 mmol) was charged into an oven-dried reaction tube equipped with a magnetic stir bar. The reaction tube was transferred into a glovebox. LiBH_4 (53 mg, 2.4 mmol) and then THF (1.25 mL) were added. The reaction tube was sealed, transferred out of the glovebox and then allowed to stir at rt. After 5 h, the reaction mixture was added to H_2O (4 mL) at 0 °C. The resulting solution was extracted with CH_2Cl_2 (8 mL). The organic layer was separated. The aqueous layer was extracted with CH_2Cl_2 (2 × 8 mL). The combined organic layers were dried with MgSO_4 , filtered and concentrated under reduced pressure. The crude product was further purified by flash

chromatography (70% EtOAc/hexanes) to afford **1** as a colorless solid; yield: 72 mg (99%). Characterization data matched previously reported information.⁷ⁿ

¹H NMR (400 MHz, CDCl₃) showed the presence of two rotamers: δ (major rotamer) = 8.02 (bs, 1 H), 7.32 (bs, 1 H), 7.06 (d, *J* = 8 Hz, 1 H), 6.90 (m, 2 H), 6.50 (d, *J* = 8 Hz, 1 H), 4.40 (d, *J* = 10 Hz, 1 H), 4.29–4.33 (m, 1 H), 3.75 (m, 1 H), 3.56 (m, 1 H), 3.18 (d, *J* = 15 Hz, 1 H), 3.04 (d, *J* = 15 Hz, 1 H), 2.92 (s, 3 H), 2.56–2.65 (m, 1 H), 0.94 (d, *J* = 7 Hz, 3 H), 0.63 (d, *J* = 7 Hz, 3 H).

¹³C NMR (100 MHz, CDCl₃): δ = 174.2, 147.8, 139.4, 122.9, 121.3, 118.0, 114.6, 106.4, 104.0, 71.1, 65.1, 55.8, 34.0, 33.0, 28.5, 21.6, 19.5.

HRMS-ESI+: *m/z* calcd for C₁₇H₂₃N₃O₂ + H: 302.1869; found: 302.1866.

Cell Growth Inhibition Assay: MTT Viability Readout

K562 or U937 cells (ATCC) were cultured in RPMI medium 1640 (Gibco) supplemented with FBS (10% v/v), penicillin (100 units/mL) and streptomycin (50 units/mL) at 37 °C, in 5% CO₂ in air in a humidified incubator. Cells were subcultured every 72–96 h (once cellular concentration reached >1,000,000 cells/mL) to a starting concentration of 200,000 cells/mL. Cell concentration was determined with a cell counter.

To assay compounds, cells were plated in plasma-treated polystyrene 96-well plates at a density of 10,000–15,000 cells/well in 50 μL of culture medium and allowed to incubate for 30 min while compound dilutions were prepared. Compounds were diluted from a 10 mM DMSO stock solution with culture medium to a concentration of 20 μM. Colchicine was used as a positive control in all experiments. Triplicate serial dilutions were then prepared in culture medium from 20 μM to 340 pM across 10 wells of a 96-well plate (diluted by factors of 3). Plates containing cells were dosed with compound (50 μL/well) to afford final assay concentrations of 10 μM to 170 pM. The maximum DMSO concentration was 0.25%. Cells were then incubated at 37 °C in 5% CO₂ in a humidified incubator for 48 h, at which time 10 μL of a 5 mg/mL solution of thiazolyl blue tetrazolium bromide (MTT; Aldrich) in cell culture medium was added to each well. The cells were allowed to incubate an additional 2.5 h, at which time they were lysed with 100 μL of a detergent solvent (20 mL Triton-X 100 (Aldrich) in 180 mL of 0.1 N HCl in *i*-PrOH).

Plates were analyzed with a VersaMax tunable microplate reader (Molecular Devices) using SoftMax® Pro version 3.1.1, reading at 570 nm and subtracting at 690 nm. The sigmoidal dose–response curves generated by plotting corrected signal vs log(drug concentration) were analyzed (least squares regression) using Prism® by GraphPad to generate EC₅₀ values. An average of several experiments is reported as indicated; experimental error indicates standard error of the mean.

Docking Studies

Computational studies were performed using the molecular modeling software Maestro (Schrödinger). Glide (grid-based ligand docking with energetics) searches were obtained to establish favorable docking interactions of indolactams **1–4** with the PKCδ C1B domain. The crystal structure of the PKCδ C1B domain (PDB code: 1PTQ) was obtained from the Protein Data Bank. Hydrogen atoms were added to the protein, and all hydrogens were energetically minimized, keeping all heavy atoms fixed. Prior to docking, the protein was prepared using the protein preparation wizard. Ligands were individually constructed using the build panel of Maestro and then conformational searches were conducted with MacroModel using an OPLS3e force

field and mixed torsional/low-mode sampling method. All ligands were docked into the active site of the PKCδ C1B domain using the extra precision (XP) mode of Glide.

Funding Information

This research was financially supported by start-up funds granted by the College of Natural Sciences and Mathematics at California State University, Fullerton. Instrumentation support was provided by the National Science Foundation MRI (CHE-1726903) for acquisition of a UPLC-MS system.

Supporting Information

Supporting information for this article is available online at <https://doi.org/10.1055/s-0039-1690198>.

References

- (1) *Protein Kinase C*; Dekker, L. V., Ed.; Springer: New York, **2004**.
- (2) (a) Whiteside, C. I.; Dlugosz, J. A. *Am. J. Physiol.* **2002**, 282, F975. (b) Vlahos, C. J.; McDowell, S. A.; Clerk, A. *Nat. Rev. Drug Discovery* **2003**, 2, 99. (c) Greenberg, D. A. *Proc. Natl. Acad. Sci. U. S. A.* **2006**, 103, 7943. (d) Etcheberrigaray, R.; Tan, M.; Dewachter, I.; Kuiperi, C.; Van der Auwera, I.; Wera, S.; Qiao, L.; Bank, B.; Nelson, T. J.; Kozikowski, A. P.; Van Leuven, F.; Alkon, D. L. *Proc. Natl. Acad. Sci. U. S. A.* **2004**, 101, 11141.
- (3) Griner, E. M.; Kazanietz, M. G. *Nat. Rev. Cancer* **2007**, 7, 281.
- (4) (a) Carter, C. A.; Kane, C. J. M. *Curr. Med. Chem.* **2004**, 11, 2883. (b) O'Brian, C. A.; Ward, N. E.; Stewart, J. R.; Chu, F. *Cancer Metastasis Rev.* **2001**, 20, 95. (c) Battaini, F. *Pharmacol. Res.* **2001**, 44, 353. (d) Ma, D. *Curr. Med. Chem.* **2001**, 8, 191. (e) Marquez, V. E.; Blumberg, P. M. *Acc. Chem. Res.* **2003**, 36, 434.
- (5) (a) Endo, Y.; Takehana, S.; Ohno, M.; Driedger, P. E.; Stabel, S.; Mizutani, M. Y.; Tomioka, N.; Itai, A.; Shudo, K. *J. Med. Chem.* **1998**, 41, 1476. (b) Wender, P. A.; Koehler, K. F.; Sharkey, N. A.; Dell'Aquila, M. L.; Blumberg, P. M. *Proc. Natl. Acad. Sci. U. S. A.* **1986**, 83, 4214.
- (6) Fujiki, H.; Sugimura, T. *Adv. Cancer Res.* **1987**, 49, 223.
- (7) (a) Endo, Y.; Shudo, K.; Furuhata, K.; Ogura, H.; Sakai, S.; Aimi, N.; Hitotsuyanagi, Y.; Koyama, Y. *Chem. Pharm. Bull.* **1984**, 32, 358. (b) Endo, Y.; Shudo, K.; Itai, A.; Hasegawa, M.; Sakai, S. *Tetrahedron* **1986**, 42, 5905. (c) de Laszlo, S. E.; Ley, S. V.; Porter, R. A. *J. Chem. Soc., Chem. Commun.* **1986**, 344. (d) Mascal, M.; Moody, C. J. *J. Chem. Soc., Chem. Commun.* **1988**, 589. (e) Masuda, T.; Nakatsuka, S.; Goto, T. *Agric. Biol. Chem.* **1989**, 53, 2257. (f) Kogan, T. P.; Somers, T. C.; Venuti, M. C. *Tetrahedron* **1990**, 46, 6623. (g) Mascal, M.; Moody, C. J.; Slawin, A. M. Z.; Williams, D. J. *J. Chem. Soc., Perkin Trans. 1* **1992**, 823. (h) Semmelhack, M. F.; Rhee, H. A. *Tetrahedron Lett.* **1993**, 34, 1395. (i) Quick, J.; Saha, B.; Driedger, P. E. *Tetrahedron Lett.* **1994**, 35, 8549. (j) Bronner, S. M.; Goetz, A. E.; Garg, N. K. *J. Am. Chem. Soc.* **2011**, 133, 3832. (k) Xu, Z.; Zhang, F.; Zhang, L.; Jia, Y. *Org. Biomol. Chem.* **2011**, 9, 2512. (l) Nathel, N. F. F.; Shah, T. K.; Bronner, S. M.; Garg, N. K. *Chem. Sci.* **2014**, 5, 2184. (m) Noji, T.; Okano, K.; Tokuyama, H. *Tetrahedron* **2015**, 71, 3833. (n) Haynes-Smith, J.; Diaz, I.; Billingsley, K. L. *Org. Lett.* **2016**, 18, 2008. (o) Nakamura, H.; Yasui, K.; Kanda, Y.; Baran, P. S. *J. Am. Chem. Soc.* **2019**, 141, 1494.

(8) Fujiki, H.; Suganuma, M.; Nakayasu, M.; Tahira, T.; Endo, Y.; Shudo, K.; Sugimura, T. *Gann* **1984**, *75*, 866.

(9) (a) Endo, Y.; Shudo, K.; Okamoto, T. *Chem. Pharm. Bull.* **1982**, *30*, 3457. (b) Nakatsuka, S.-i.; Masuda, T.; Sakai, K.; Goto, T. *Tetrahedron Lett.* **1986**, *27*, 5735. (c) Mari, M.; Bartoccini, F.; Piersanti, G. *J. Org. Chem.* **2013**, *78*, 7727.

(10) Choi, D. W.; Hartley, D. M. US5292765A, **1994**.

(11) Kawai, T.; Ichinose, T.; Endo, Y.; Shudo, K.; Itai, A. *J. Med. Chem.* **1992**, *35*, 2248.

(12) Mendoza, M.; Rao, N.; Tran, U.; Castaneda, C.; Billingsley, K. L. *Tetrahedron* **2019**, *75*, 4337.

(13) Angelini, E.; Balsamini, C.; Bartoccini, F.; Lucarini, S.; Piersanti, G. *J. Org. Chem.* **2008**, *73*, 5654.

(14) (a) Kortmansky, J.; Schwartz, G. K. *Cancer Invest.* **2003**, *21*, 924. (b) Kollár, P.; Rajchard, J.; Balounová, Z.; Pazourek, J. *Pharm. Biol.* **2014**, *52*, 237.

(15) Nakagawa, Y.; Irie, K.; Yanagita, R. C.; Ohigashi, H.; Tsuda, K. *J. Am. Chem. Soc.* **2005**, *127*, 5746.

(16) Irie, K.; Isaka, T.; Iwata, Y.; Yanai, Y.; Nakamura, Y.; Koizumi, F.; Ohigashi, H.; Wender, P. A.; Satomi, Y.; Nishino, H. *J. Am. Chem. Soc.* **1996**, *118*, 10733.

(17) Kawai, T.; Ichinose, T.; Takeda, M.; Tomioka, N.; Endo, Y.; Yamaguchi, K.; Shudo, K.; Itai, A. *J. Org. Chem.* **1992**, *57*, 6150.

(18) Hesek, D.; Lee, M.; Noll, B. C.; Fisher, J. F.; Mobashery, S. *J. Org. Chem.* **2009**, *74*, 2567.